Acta Crystallographica Section D
**Biological Crystallography**
ISSN 0907-4449

# High-throughput crystal-optimization strategies in the South Paris Yeast Structural Genomics Project: one size fits all?

**Nicolas Leulliot,[a]* Lionel Trésaugues,[a] Michael Bremang,[a] Isabelle Sorel,[a] Nathalie Ulryck,[a] Marc Graille,[a] Ilham Aboulfath,[a] Anne Poupon,[b] Dominique Liger,[a] Sophie Quevillon-Cheruel,[a] Joël Janin[a] and Herman van Tilbeurgh[a,b]***

[a]Institut de Biochimie et de Biophysique Moléculaire et Cellulaire (CNRS–UMR 8619), Université Paris-Sud, Bâtiment 430, 91405 Orsay, France, and [b]Laboratoire d'Enzymologie et Biochimie Structurales (CNRS–UPR 9063), Bâtiment 34, 1 Avenue de la Terrasse, 91198 Gif sur Yvette, France

Correspondence e-mail: nicolas.leulliot@ibbmc.u-psud.fr, herman.van-tilbeurgh@ibbmc.u-psud.fr

Received 22 July 2004
Accepted 13 January 2005



Crystallization has long been regarded as one of the major bottlenecks in high-throughput structural determination by X-ray crystallography. Structural genomics projects have addressed this issue by using robots to set up automated crystal screens using nanodrop technology. This has moved the bottleneck from obtaining the first crystal hit to obtaining diffraction-quality crystals, as crystal optimization is a notoriously slow process that is difficult to automatize. This article describes the high-throughput optimization strategies used in the Yeast Structural Genomics project, with selected successful examples.

## 1. Introduction

Structural genomics (SG) initiatives around the world aim to bridge the gap between amino-acid sequence and three-dimensional structure of the corresponding protein by filling the catalogue of protein folds. This has created a technological driving force towards automation of most of the steps starting from gene cloning, protein expression and purification, to three-dimensional structure determination either by NMR or X-ray crystallography. Every step in this process needs as much automatization as possible in order to process a large number of proteins in parallel.

Since the beginning of SG projects, crystallization has been recognized as one of the major bottlenecks of the whole structure-determination processes. This has driven the pilot structural genomics projects to implement robotics to automatize the set up of initial crystal screens. The use of pipetting robots to fulfil this task has been described and reviewed elsewhere (Walter *et al.*, 2003; Bodenstaff *et al.*, 2002). The use of robots has the double advantage of accelerating the set-up of crystallization trials and of reducing the amount of protein necessary, which enables more proteins to be screened per day and more trials to be performed per protein.

Crystallization robots have had a tremendous impact on the success rate of obtaining crystals. Results from the South Paris Yeast Structural Genomics Project (YSG; http://genomics.eu.org; Quevillon-Cheruel *et al.*, 2003), as well as from other SG projects around the world, show that the success rate of crystallization is relatively high, with around 50% of proteins entering crystal trials giving crystals of some sort. However the structures of only half of these proteins have been solved. Indeed, the first hits usually provide crystalline precipitate, needles, thin plates, micro- or polycrystals, that are not suitable for diffraction experiments. It was soon realised that (i) increasing the number of conditions was not an appropriate method to obtain well ordered, single crystals of suitable size and (ii) the crystal optimization towards diffraction quality crystals is difficult to automatize.

Consequently, the crystallization bottleneck has shifted from screening setup to optimization of crystallization conditions. Optimizing crystal conditions implies a more classical approach where one tries first to reproduce the crystal hit manually and then to vary the crystallization conditions (precipitant conditions, pH, ionic strength . . . ). The 'one size fits all' protocol applied in structural genomics breaks down at this stage as each protein crystal optimization is unique. The main problems to be addressed are that (i) optimization setups require tailor-made solutions to be prepared for each protein, (ii) the outcome of the crystallization trial is influenced

by the change in experimental set-up: going from sitting drop to hanging drop, increasing the drop volume, changing the mixing mode of protein/mother liquor, (iii) reproducing crystal hits from commercial screens with home-made solutions can also be of some concern, (iv) optimization is a multiple step procedure: every decision depends on the outcome of the previous crystallization experiment, which can take days or weeks to equilibrate and give positive or negative results, (v) between each experiment the protein sample ages, which can have detrimental effects on the outcome of crystallization, and forces one to plan and perform all the experiments in a short lap of time.

In this paper, we describe the high throughput crystal optimization strategies adapted in our South Paris Yeast Structural Genomics Project (YSG). The focus of our strategy is to design a 'standard' optimization protocol applicable to all the proteins and that can be easily automated in order to streamline the crystal optimization process. An overview of results of these techniques with proteins of the YSG project will be presented.

## 2. Experimental methods

The expression and purification of the proteins used in this work have been described elsewhere (Quevillon-Cheruel *et al.*, 2005). The Greiner-BioOne sitting-drop vapour-diffusion 96-well plates are used for the screening and optimization trials. Commercial screens from Jena Bioscience, Hampton and Nextal are used for the initial screens.

Two liquid-dispensing robots are used in the laboratory. The Tecan Genesis is used for dispensing mother liquor solutions in the crystallization well reservoir (100–150 µl) and setting up high-volume crystallization trials (0.5–2 µl). A volume of protein is pipetted by the eight needles, followed by the addition of the equivalent volume of precipitant solution and deposited on the cups of the crystallization plate. The protein and precipitant can either be homogenized by successive aspiration/distribution or deposited without further mixing. The process is repeated 12 times to fill the plate. As three different crystallization cups are available, three different protein solutions can be tested in parallel, usually three different protein concentrations, or protein solutions differing in composition (purification, buffer, pH, ionic strength or ligands).

The Cartesian Microsys is used to set up low-volume crystallization drops in plates prefilled by the Tecan robot (Sulzenbacher *et al.*, 2002). Routinely, volumes of 100 nl are used for both the protein and the precipitant, but volumes of 50 nl for each component have successively been used. However, this last experimental setting can be problematic with high viscosity precipitants. The precipitant is deposited first in all the cups, followed by line dispensing of the protein solution in the 96 wells. No control is available of the protein/precipitant mixing other than that achieved by the impact of the protein drop that is ejected into the precipitant drop. The dispensing apparatus is enclosed in a humidity-controlled chamber to limit drop evaporation.

## 3. Manual optimizations

Once a crystal hit is found, a typical optimization strategy consists in exploring the physico-chemical conditions around the original hit. This commonly involves setting up line gradients around the precipitant concentration, the pH or the concentration of the additive or salt, the aim being to on one hand reproduce the crystal hit and on the other hand produce higher quality single crystals. If this fails, replacing any of the original ingredients, adding arbitrary reagents or modifying the experimental set-up (drop size, protein/precipitant ratio . . . ) is generally used. Manual optimizations are performed in Limbro plates with typically 1 + 1 µl protein/precipitant deposited on siliconized cover slips with wells filled with 500–1000 µl precipitant.

The most prominent setback is over-nucleation in the drop, leading to microcrystals or polycrystalline matter. In these cases, an extensive exploration of crystallization conditions is required. It aims to modulate protein solubility, to influence drop equilibration kinetics and to separate crystal nucleation and growth. Two strategies employed with success in another study (Chayen & Saridakis, 2002) are regularly used in our optimization procedures, because they are easy to set up, they use the same solutions prepared for the manual approach and can therefore be used in parallel with classic optimization.

Firstly one can limit the evaporation kinetics by adding a layer of oil on top of the reservoir solution, with aim of limiting nucleation and favouring growth of a limited number of large crystals (Chayen, 1997). The procedure simply involves adding a layer of 200 µl of a 1:1 mixture of paraffin and silicon oil on top of a manually set-up crystallization optimization trials exploring the conditions around the original hit. Alternatively, one can use only the original hit condition and set-up a 'gradient' of the oil permeability barrier over multiple wells, achieved by varying the ratio of paraffin/silicon oil or by varying the layer thickness between the different wells. In case the original condition contains reagents that are not available, or if home-made solutions do not give the same results as the commercial solution, this last method has the advantage of performing the optimization with the original kit solution.

The second method involves crystallizing in gelled media. Hampton Silicate gels were used with the same conditions as the manual optimization or with the original kit solution. Crystallization in gels reduces convection and slows down the equilibration kinetics, thereby favouring the formation of single crystals (Chayen, 2003). The drawback of this method lies in the time needed to set up the experiment.

## 4. Automated optimization

### 4.1. Optimization in 96 wells

The main drawback in manual optimization is the time needed to set up the trials: preparation of the precipitant solutions, pipetting, dispensing and mixing the protein/precipitant drop and visualization of the results. In order to design a standard optimization protocol that can be integrated on the automated pipetting platform, we assume that the crystal hit contains components that can be classified in four different categories: a main precipitant, a buffer, a salt and an additive. This mix will hereafter be referred to as the 'hit solution'.

### 4.2. Fine grid exploration of the crystallization conditions: two-dimensional and three-dimensional screens

Exploration of the crystal conditions from the initial screen is performed by setting up fine grid screens in which the concentration of two components of the hit solution are varied (Lartigue *et al.*, 2003). The Tecan pipetting robot is supplied with four stock solutions (P1, P2, A1, A2). P1 and P2 correspond to the hit solution minus one component and vary by the concentration of one of the components (usually the precipitant). A1 and A2 correspond to the component left out of P1 and P2. The A1 and A2 solutions will either explore a certain pH range of the buffer or a chosen concentration range of the salt or additive. The Tecan robot has been programmed to automatically set-up two-dimensional grid screens of various sizes, 12 × 8, 8 × 8, 6 × 8, by mixing in each well the appropriate amount of the

four solutions (Fig. 1*a*). The stock-solution concentrations are calculated so that they are at the desired concentration after the four way mix. The drops can then be deposited either by the Tecan or Cartesian robot.

Three components can also be explored in a single experiment: six 4 × 4 grid screens can be set up on a single 96-well plate. In each of these two-dimensional screens, the concentration of a third component can be varied thereby creating a three-dimensional screen (Fig. 1*b*). If a fourth component can be added to the protein solution and varied in the three protein drops of each well (possible only for non volatile components) then a four-dimensional exploration of parameter space is achieved.

### 4.3. Additive/pH/salt screens

Grid screens can be used to define a region in parameter space which is stable in respect to variations of the concentration (or pH) of each of the components, facilitating the reproducibility of subsequent trials with a 'refined hit' solution. In some cases, this optimization is sufficient to obtain a monocrystal. Otherwise, most optimization trials have to be performed by extending the search to other parameters.

Addition of another component, often referred to as additive screening, can greatly enhance the crystallization process. As the *a priori* choice of the type of additive is not always possible, the method is based on trial and error and is therefore ideally suited for automation. We have designed an additive screen containing 96 additives spanning different chemical properties: mono- and divalent salts, polymers, solvents and small molecules. The crystallization plate is set up automatically with the Tecan robot or manually with a multipipette from the additive screen stored in 96 deep well plates and one stock solution of the refined hit solution. If there is an additive in the hit solution, it can be either removed or kept for the additive screen. If a suitable additive is found, the process can be iterated to find a second additive.

The type of salt in the crystallization trial can also be varied on the same principle with a 'salt screen' containing 48 salts at two different concentrations, providing 96 conditions to be mixed with the refined hit solution where the salt component has been left out.

If a large range of pH values are to be tested, a 'pH screen', provides 48 solutions, buffered with different compounds at 48 different pH values from 2.2 to 11 by 0.2 pH unit steps (such as the Hampton pHScreen), to be mixed with a refined hit solution where the buffer component has been left out.

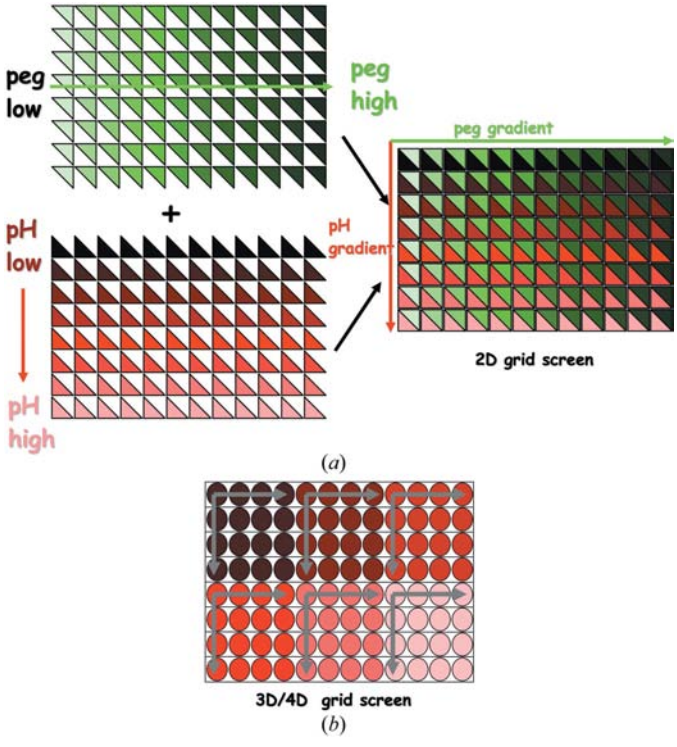


**Figure 1**
(*a*) Two-dimensional grid screens. The additive concentration, or pH gradient, is disposed on a vertical grid (shades of red) from the two stock solutions, while the precipitant mix is disposed on a horizontal grid (shades of green). The four way mix effectively creates a two-dimensional gradient exploring all the combinations of the two parameters. (*b*) Three-dimensional grid screens. Six 4 × 4 grid screens are set-up on one plate. In each two-dimensional grids, the concentration of a third component in the mother mix is varied (shades of red) creating the third dimension of the screen. Alternatively, six totally different conditions can be optimized in parallel. A colour version of this figure is available in the onlne edition of the journal.

### 4.4. Cryo-screens

Once a suitable condition is found and mono-crystals are available, one further rate-limiting step towards structure solution is the determination of suitable cryoprotectant solutions. This is a time- and crystal consuming process where besides obvious crystal cracking or dissolving in the cryo-protectant solution, the only real test is collecting a few diffraction images and checking for ice rings and monitoring crystal mosaicity.

The YSG cryo-screen consists of 12 different cryo-protectants at four different concentrations. The kit is used like the additive screens but is designed so that the cryoprotectant contributes from 1% to 30% of the final solution. Results are used in the following way.

(i) If the protein crystallizes in a high cryoprotectant concentration, the protein can probably be transferred straight from the drop into liquid nitrogen without the need for intermediate soaks

(ii) If a suitable crystal grows in a low concentration of a cryoprotectant, the crystal is transferred in increasing concentrations of that cryoprotectant until the desired protection is achieved. The fact that the crystal has grown from a low percentage of cryoprotectant solution generally reduces the osmotic shock occurring often during the transfer to higher concentrations of that same cryoprotectant. It can be noted that the solutions for the different baths are pre-prepared in the wells of the 'cryoscreen'

(iii) If no suitable monocrystals grow in the 'cryo kit', the outcome of the drops can nevertheless be used to make decisions as to the best cryoprotectant to test. Cryoprotectants in which poly crystals, or crystalline precipitate grow are good candidates. Cryoprotectants giving clear drops indicate that care must be taken as the increased solubility of the protein in the precipitant might lead to the crystal melting in the different cryoprotectant baths. Heavy precipitate or phase separations indicate that the cryoprotectant is inappropriate.

## 5. Results and discussion

The optimization strategies and screens have not been extensively tested, for example by monitoring the crystallization behaviour of model proteins, but they have proved so successful that they are used in the optimization of all the proteins of the YSG project and of the proteins of collaborators using the YSG platform. The following section presents some of the results and experience gained using these strategies. We will only present results on proteins whose structure has finally been solved.

### 5.1. Oils and gels

Fig. 2(*a*) shows the initial crystal optimization trials of the yeast YML079w gene product. The thin stacked platelets resisted all efforts in manual optimization trials, although single isolated crystals sometimes appeared which could be harvested and on which full datasets could be recorded. In Figs. 2(*b*) and 2(*c*) the same precipitant solutions have been used in manual trials with respectively a layer of oil on top of the reservoir (Fig. 2*b*) and crystal grown in gels (Fig. 2*c*). Both methods show a spectacular improvement in crystal size and thickness.

In the case of oils, although stacked platelets are still present in most drops, the delay in the equilibration kinetics enables more thicker crystals to appear. The crystals grown in gels take several weeks to appear (compared to a few days) and are amongst the largest and thickest crystals obtained. Unfortunately, diffraction of these crystals showed that they were extremely mosaic, probably the result of regular stacking of slightly shifted monocrystalline plates. Once again, this highlights the fact that exterior aspect of crystals can be misleading. The structure has been solved in another crystal form (manuscript in preparation).

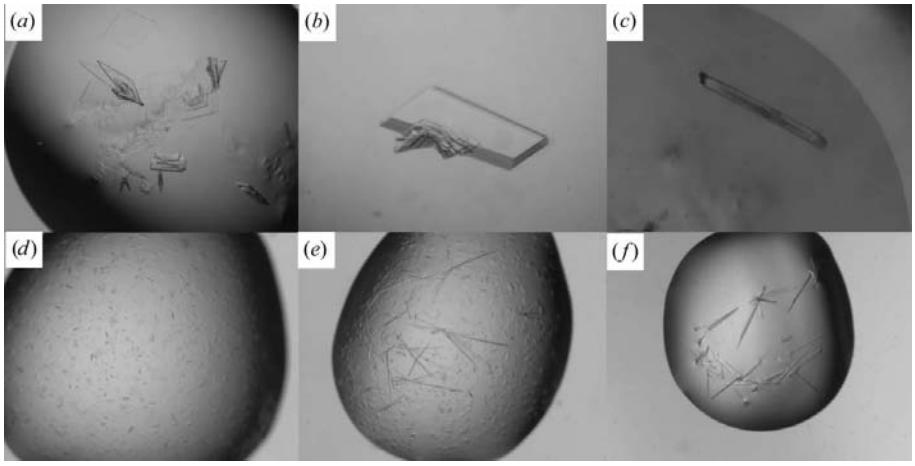


**Figure 2**
(*a*) Yeast YML079w gene product of the YSG project crystallized in 20% PEG 4000, 0.1 *M* sodium citrate pH 6.5. This condition gives thin, stacked platelets that resisted all optimization efforts. (*b*) Same conditions as (*a*), with a 200 µl oil mix of paraffin/silicon on top of the well reservoir. (*c*) Same conditions as (*a*), grown in silica gel. (*d*) Yeast YCR004*c* gene product of the YSG project crystallized in 18% PEG 4000, 0.2 *M* $MgCl_2$, 0.1 *M* NaCaco pH 6. (*e*) Same condition as (*d*) with a 200 µl layer of oil on top of the reservoir, leading to the coexistence of the microcrystals with a second crystal form. (*f*) same condition as (*e*) with 300 µl layer of oil on top of the reservoir supported the growth of the larger rod-like crystals.

Fig. 2(*d*) shows the small crystals of YCR004c that could be obtained by varying the conditions around the initial hit. These crystals grew in 2 d and did not diffract. An oil barrier was therefore used in an attempt to slow the nucleation rate. In drops set up with a 200 µl oil barrier (on top of a 1 ml reservoir solution), two crystal forms grew after 4 d: the original hexagonal microcrystals and long needle/rod-like crystals (Fig. 2*e*). The balance between the quantities of the two crystal forms could be influenced by the thickness of the oil layer: at 300 µl, only the rod-like crystals grew in 7 d (Fig. 2*f*).

### 5.2. Two-dimensional and three-dimensional screens

After an initial hit is found, the first optimization screens usually explore the precipitant concentration and buffer pH, as the crystallization has been found to be most sensitive to these parameters. Exploration of initial successful conditions has proven to be critical in reproducing some of the hits from commercial screens. Indeed, the stock solutions of home-made and commercial solutions are different, the final pH of the hit solution is often found to be different from the expected one (Wooh *et al.*, 2003), and the screen condition might have been subject to evaporation or contamination during the multiple times the tube was opened to fill plates. Although grid screens have always been used in manual setups, the limited amount of protein available necessarily reduces the amount of parameters that can be varied and one generally chooses to set up line gradients where only one parameter is varied at a time. Our strategy presents a gain in time (both in well solution setup and protein dispensing), and benefits from reduced protein use which permits the exploration of crystallization space on a finer and more extensive grid. Automation also makes this step of the optimization procedure fit in the high-throughput crystallization pipeline.

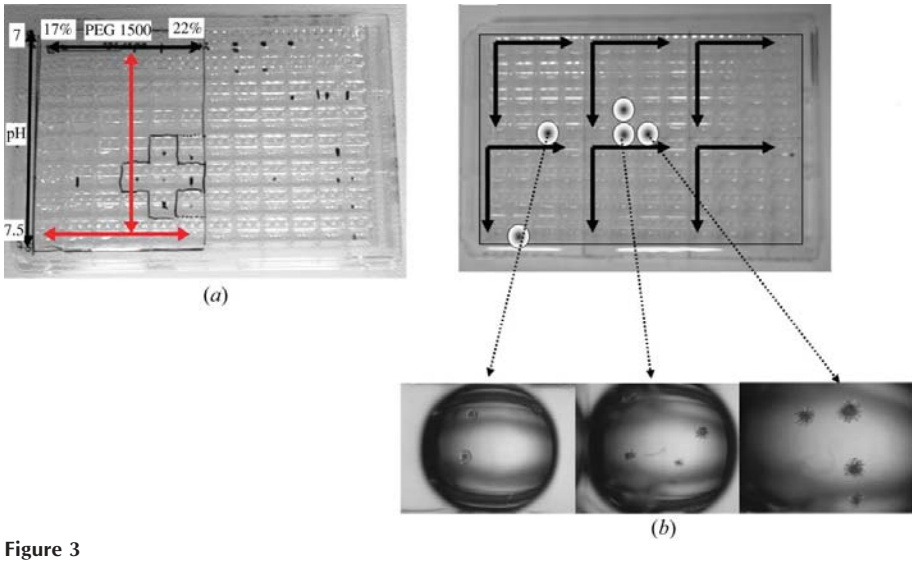


**Figure 3**
(*a*) Two-dimensional optimization screen. The original hit was found in 20% PEG 1500, 0.1 *M* Na HEPES pH 7–7.5. The two-dimensional grid is set up between 17–22% PEG 1500 and 0.1*M* Na HEPES pH 7–7.5. The nucleation zone is boxed. A traditional manual line gradient would have explored the region marked by double red arrows, which might have missed the crystal and led to inconclusive results. (*b*) Three-dimensional optimization screen. Six 4 × 4 grid screens explore the precipitant/pH conditions (1.2–1.6 ammonium sulfate/Tris pH 7–8) with different glycerol and salts identified as promising additives in the additive screen. In each grid six different conditions are sampled in parallel, from left to right, bottom to top: 5% glycerol/0.3 *M* NaCl, 10% glycerol/0.2 *M* NaCl, 5% glycerol/0.2 *M* NaCl/10 m*M* spermidine, 5% glycerol/0.3 *M* Na acetate, 0.2 *M* NaCl, 5% glycerol/0.2 *M* Mg acetate. A colour version of this figure is available in the onlne edition of the journal.

Fig. 3(*a*) shows an example of reproduction of protein crystals achieved in a region corresponding to a narrow range of precipitant/pH combination by two-dimensional

screens. The original hit was found from JBS screen (20% PEG 1500, 0.1 *M* Na HEPES pH 7.5). In manually set-up line gradients where one varies one parameter at a time while fixing the others (here a PEG gradient at fixed pH or a pH gradient at fixed PEG concentration, double arrows in Fig. 3*a*), the crystal producing conditions could easily have been missed, while the crystal nucleation zone is clearly defined in the two-dimensional screen.

Three-dimensional screens, exploring three parameters of a hit condition, have also shown themselves to be very promising in defining a stable region of crystal growth. In Fig. 3(*b*), the three-dimensional gradient of a protein–protein complex is shown, with the conditions giving crystals indicated by red circles. Each 4 × 4 two-dimensional gradient (precipitant *versus* pH) is set-up with a solution differing in composition: a different combination of glycerol and salt concentrations, additives and different salts, thereby testing in parallel and on a fine grid six conditions that looked promising in additive screens. The rod extruding from the bigger urchin-like crystals were separated and the structure of the protein–protein complex was solved by molecular replacement.

### 5.3. Additive screens

Target 91 (YHR049w) crystallizes as small long needles. Two-dimensional screens, additive and salt screens were set up in parallel as sufficient protein was available. A few results of the additive screen are shown in Fig. 4 with the original hit as the control. It can be seen that a number of additives lead to significant improvement in crystal number and size. Similar size crystals could finally be obtained with and without additive. However, diffraction tests showed that crystals grown from original hits (Fig. 4*g*) did not diffract, whereas crystals grown in the presence of 0.1 *M* $LiCl_2$ (Fig. 4*e*) diffracted to 2.4 Å resolution on the ID23 beamline (ESRF, Grenoble, France). This is thought to result from melting of the 'native' crystal during the transfer in the solutions containing cryo-protectants, while the crystals grown in the presence of some of the additives were more stable. The structure has been solved by single anomalous diffraction (manuscript in preparation).

In the case of yeast chorismate synthase, additive screening did not improve crystal quality. However, 0.1 *M* EDTA was found to accelerate the appearance of the crystals from approximately two weeks to less than 4 d. This enabled conditions to be refined on a shorter time scale. The structure has been solved by single anomalous diffraction (Quevillon-Cheruel *et al.*, 2004).

The first screens of target L1 (protein domain) identified one condition as having crystalline precipitate and possibly some quickly disappearing needles. Two-dimensional optimization of precipitant concentration and buffer pH was not sufficient to produce diffraction-quality crystals. The manual approach using a layer of oil showed some promise with coarser grained crystalline precipitate. This original hit condition was then used in an additive screen. The control and all but one additive yielded very fine crystalline precipitate, while in the drops containing polypropylene glycol 400 (PPG400), large monocrystals were observed after 7 h (Fig. 5*a*). It can also be noted that PPG400 was not miscible with the precipitant (ammonium sulfate), creating a layer on top of the well. The layer of PPG400 might have a role similar to the oil layer in slowing down the equilibration kinetics. This highlights the fact that chemical compatibility of the additives and the precipitants is not mandatory. The crystals grown in these conditions were fragile and degraded in the drops after 8 h. Iteration of the additive screen, with the PPG400 included, identified ethylene glycol and glycerol as a second additive that were able to produce larger and more stable monocrystals (Fig. 5*b*). Glycerol was also used as the cryoprotectant. The need for the most stable crystal was crucial as the structure has been solved by heavy-atom soaking (manuscript in preparation).

Iterative additive screens were also the key to the success of crystallization of Target 228. The initial crystal hit gave brushy needles (Fig. 5*c*). In the next optimization step, a salt screen identified KCl as an effective replacement for the original $MgCl_2$. The change in salt gave rise to small monocrystalline needles (Fig. 5*d*). The optimization procedure was iterated with this new solution and was used in an additive screen. Guanidine, in combination with KCl, was found to improve the size of the needles (Fig. 5*e*), which permitted a full data set on these crystals to be recorded. The structure was solved by single anomalous diffraction (manuscript in preparation).

### 5.4. Cryo-screens

Refinement of the initial hit of target 48 (YHR029c) enabled monocrystals of reasonable size to be obtained. However, the transfer to baths containing cryoprotectants was in general destructive. After

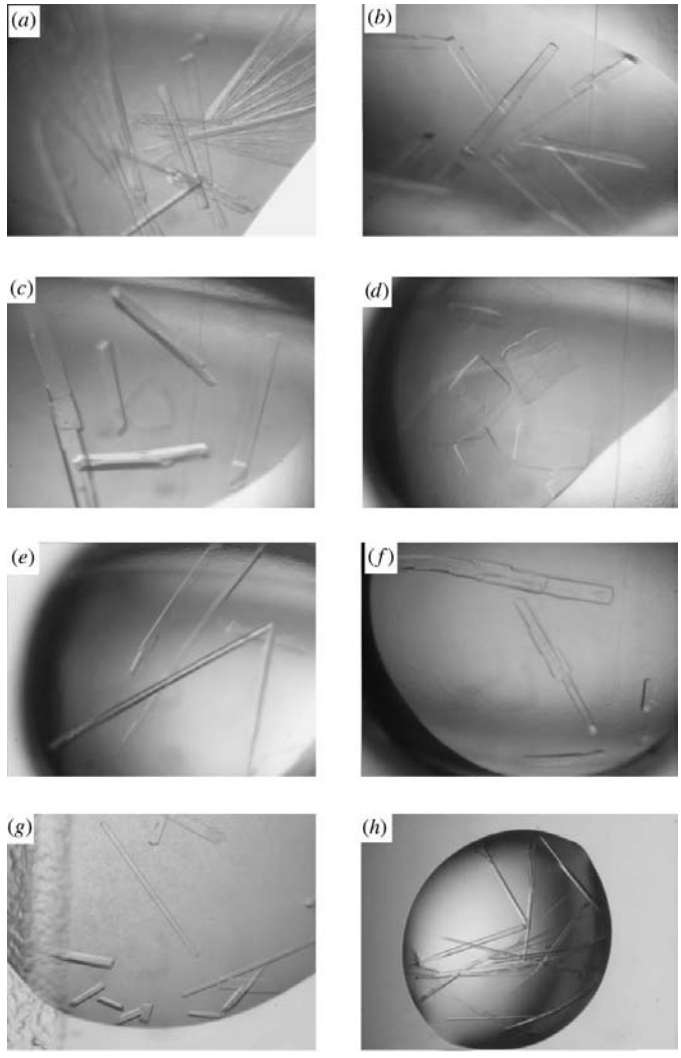


**Figure 4**
Results from the additive screen of target 91. The control condition is shown in (*a*). Different crystal habits, or size are observed with (*b*) 3% dioxane, (*c*) 4% *n*-propanol, (*d*) 3% 1,8-diaminooctane, (*e*) 10 m*M* EDTA, (*f*) 10 m*M* urea. (*g*) The optimization of the original conditions yielded suitable sized crystals that did not diffract. (*h*) Optimization of the crystals with 0.1 *M* $LiCl_2$ as additive yielded well diffracting crystals.

many trials, a data set was recorded on ID14-1 (ESRF, Grenoble, France) at 3.1 Å resolution. Using this condition in a 'cryo-screen' it was observed that most cryoprotectant additives did not favour crystal growth. Glycerol inhibited crystal growth at 1–15% but full size crystals grew at 30%. At this concentration, the solution is already cryoprotected and crystals could be flash-frozen directly into liquid nitrogen. The crystals diffracted to 2.2 Å resolution on the laboratory Rigaku rotating-anode generator. The structure has been solved by multiple anomalous diffraction (D. Liger, work submitted).

Cryo-protection of target 205 (YIR029w) yielded an unexpected result. Initially, crystals grown and cryoprotected in hexanediol were used and a full multiple-wavelength anomalous dispersion data set recorded. Unfortunately, the arrangement of the molecules in the asymmetric unit gave rise to translational symmetry (noncrystallographic axis parallel to crystallographic axis), which hindered our attempts to find the selenium sites. However, crystals grown and frozen in glycerol crystallized in another space group and the structure was solved (Leulliot *et al.*, 2004).

## 6. Conclusion

The optimization strategies we have outlined can be used to define a standard, one size fits all, optimization procedure. Once a crystal hit is found, a two-dimensional or three-dimensional grid screen can be set up to reproduce and refine the original hit. Once a stable crystal growing zone is found, additive and salt screens can be used to further refine the conditions. The grid screens/additive screens can be iterated until a satisfactory result is found. This solution is then used in a cryo-screen to find suitable cryo-protectants. If needed further large scale production can be set up by the robots to avoid the problems of reproducing the crystals by hand. In this last step Greiner low profile plates are used to simplify crystal harvesting. Gels or oils can be introduced at any stage of the process. If protein sample is limited, the design of the kits also makes it possible to use a subset of each kit on one plate, for example to test 48 additives, 16 pH values and 32 salts. Of course, if protein quantity permits, all the complete screens can be employed in parallel, and iterated only if necessary.

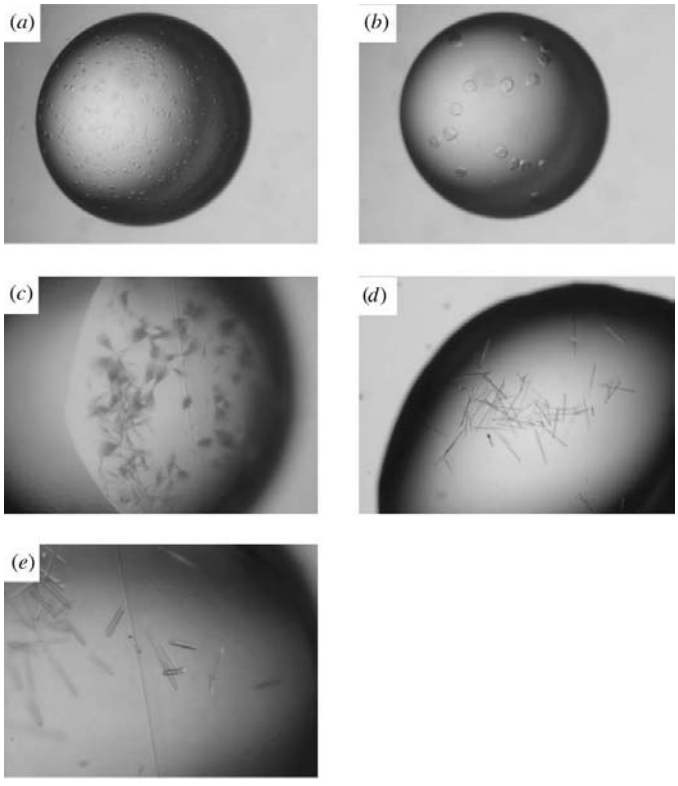


**Figure 5**
(*a*) Crystals after the first round of an additive screen on protein target L1. The initial hit in 2.0 *M* ammonium sulfate, 0.1 *M* Na acetate pH 4.6 gave an overnucleated drop where one could distinguish microcrystals (not shown). Addition of 4% poly propylene glycol 400, leads to cubic crystals to form. (*b*) Iteration of the additive kit with a solution containing 2.0 *M* ammonium sulfate, 0.1 *M* Na acetate pH 4.6, 4% PPG400. Larger crystals are formed in the drop containing 3% ethylene glycol. Glycerol could also be used as an additive with the same effect and was also used as the cryoprotectant. (*c*) Needle clusters of Target 228 obtained in the initial crystal screen 16% PEG 4000, 0.1 *M* $MgCl_2$, 0.1 *M* Tris pH 8.5. (*d*) Condition from salt screen, where 0.1 *M* $MgCl_2$ was replaced by 0.1 *M* KCl: thin needles are produced. (*e*) Screening of additives using condition (*d*) showed that 0.1 *M* guanidine improved notably crystal size.

The YSG optimization strategy benefits in terms of time and reproducibility from automated set-up of all the gradients, dilutions and mixes, with only a minimal number of solutions that have to be prepared by hand, and from the actual protein/precipitant drop dispensing. It also represents a gain in terms of amounts of protein through use of nanolitre drop dispensing technologies which enables a more extensive set of optimization conditions to be explored before the final scale up for crystal production for the diffractometer. Indeed the time and protein gained using this strategy can be employed to optimize several different conditions in parallel.

The fact that automated set-up raises by an order of magnitude the number of experimental drops that have to be visualized could displace the bottleneck from drop set-up to visualization. However, the use of a storage and visualization robot, such as our BioSTORE-200 robot (http://www.biotom.net), to periodically take pictures of all the drops made in 96-well plates, removes the time-consuming step of drop inspection through a binocular microscope. Storage space is also reduced by using the 96-well plates. Data management is also made easier compared with traditional optimization strategies because every step fits in a pre-defined experiment where only the hit solution is protein specific. In our electronic laboratory lab book (*HalX*, freely available at http://halx.genomics.eu.org, see Prilusky *et al.*, 2005), the screens are predefined making data storage and mining a straightforward task.

The need for efficient crystals optimization strategies is justified by the upstream biochemical efforts to provide proteins for crystallization trials. The YSG optimization strategies have proved very successful in producing a large quantity of mono-crystals of suitable size. But as the real test for crystal quality is diffraction, the future might prove to us that we are moving to another bottleneck, *i.e.* testing the crystals on the diffractometer. The automation of synchrotron beamlines, and especially the availability of crystal mounting robots, is of special interest to the SG community. Recently, staff of the FIP beamline (BM30A, ESRF) has designed a procedure able to observe the diffraction of crystal *in situ* by shooting directly into the drops of Greiner boxes (Jacquamet *et al.*, 2004), which could make possible to test the effect of optimization procedures directly in reciprocal space.

This work is supported by grants from the Ministère de la Recherche et de la Technologie (Programme Génopoles) and Association pour la Recherche sur le Cancer (to MG).

## References

Bodenstaff, E. R., Hoedemaeker, F. J., Kuil, M. E., de Vrind, H. P. & Abrahams, J. P. (2002). *Acta Cryst.* D**58**, 1901–1906.
Chayen, N. E. (1997). *Structure*, **5**, 1269–1274.

Chayen, N. E. (2003). *J. Struct. Funct. Genomics*, **4**, 115–120.
Chayen, N. E. & Saridakis, E. (2002). *Acta Cryst.* D**58**, 921–927.
Jacquamet, L., Ohana, J., Joly, J., Borel, F., Pirocchi, M., Charrault, P., Bertoni, A., Israel-Gouy, P., Carpentier, P., Kozielski, F., Blot, D. & Ferrer, J. L. (2004). *Structure*, **12**, 1219–1225.
Lartigue, A., Gruez, A., Briand, L., Pernollet, J. C., Spinelli, S., Tegoni, M. & Cambillau, C. (2003). *Acta Cryst.* D**59**, 919–921.
Leulliot, N., Quevillon-Cheruel, S., Sorel, I., Graille, M., Meyer, P., Liger, D., Blondeau, K., Janin, J. & van Tilbeurgh, H. (2004). *J. Biol. Chem.* **279**, 23447–23452.
Prilusky, J., Oueillet, E., Ulryck, N., Pajon, A., Bernauer, J., Krimm, I., Quevillon-Cheruel, S., Leulliot, N., Graille, M., Liger, D., Trésaugues, L., Sussmann, J. L., Janin, J., van Tilbeurgh, H. & Poupon, A. (2005). *Acta Cryst.* D**61**, 671–678.
Quevillon-Cheruel, S. *et al.* (2003). *J. Synchrotron Rad.* **10**, 4–8.
Quevillon-Cheruel, S., Collinet, B., Trésaugues, L., Minard, P., Henkes, G., Aufrère, R., Blondeau, K., Bettache, N., Zhou, C.-Z., Liger, D., Janin, J., Poupon, A. & van Tilbeurgh, H. (2005). In the press.
Quevillon-Cheruel, S., Leulliot, N., Meyer, P., Graille, M., Bremang, M., Blondeau, K., Sorel, I., Poupon, A., Janin, J. & van Tilbeurgh, H. (2004). *J. Biol. Chem.* **279**, 619–625.
Sulzenbacher, G. *et al.* (2002). *Acta Cryst.* D**58**, 2109–2115.
Walter, T. S., Diprose, J. J., Brown, M. P., Owens, R. J., Stuart, D. I. & Harlos, K. (2003). *J. Appl. Cryst.* **36**, 308–314.
Wooh, J. W., Kidd, R. D., Martin, J. L. & Kobe, B. (2003). *Acta Cryst.* D**59**, 769–772.